Numerical analysis of flow resistance and heat transfer in the transitional regime of pipe flow with twisted-tape turbulators

IOP Conf. Series: Journal of Physics: Conf. Series **923** (2017) 012033 doi:10.1088/1742-6596/923/1/012033

Numerical analysis of flow resistance and heat transfer in the transitional regime of pipe flow with twisted-tape turbulators

R Rossi[1], L Cattani[3], A Mocerino[4], F Bozzoli[1,3], S Rainieri[1,3], R Caminati[2] and G Pagliarini[1]

[1] CIDEA Interdepartmental Centre, University of Parma, Parco Area delle Scienze 181/A, I-43124 Parma, Italy
[2] Be.Tube S.r.l., Via Cicagna 52, 47522, Cesena (FC), Italy
[3] SITEIA.PARMA Interdepartmental Centre, University of Parma, Parco Area delle Scienze 181/A, I-43124 Parma, Italy
[4] Department of Industrial Engineering, University of Parma, Parco Area delle Scienze 181/A, I-43124 Parma, Italy

E-mail: fabio.bozzoli@unipr.it

Abstract. In this paper, we present the numerical analysis of the fully developed flow and heat transfer in pipes equipped with twisted-tape inserts in the laminar to transitional flow regime. The flow Reynolds number ranges from 210 to 3100 based on the pipe diameter, whereas the Prandtl number of the working fluid, a 40% mixture of water and ethylene glycol, is about 45 at the average film temperature. The numerical study is carried out via Scale Adaptive Simulations (SAS) where the k-ω SST model is employed for turbulence modeling. Using SAS and low-dissipation discretization schemes, the present study shows that it is possible to capture the transition from the laminar regime to the pulsating or pseudo-laminar flow regime induced by the twisted-tape at low Reynolds numbers, as well as the transition to moderate turbulent regime at the higher, yet non-turbulent for smooth pipes, range of Reynolds numbers. Numerical results, validated against experiments performed in a dedicated test rig, show very good agreement with measured data and an increase of the friction factor and Nusselt number in the range of 4 to 7 times and 6 to 15 times, respectively, of the values for an empty pipe.

1. Introduction

The use of heat transfer augmentation techniques is a common practice when heat exchangers operate with high-viscosity fluids and thus at low Reynolds numbers, where the heat transfer is minimal due to the persistence of the laminar flow regime. The urgency on heat transfer enhancement is also driven by the tendency in many industrial, commercial and domestic applications (e.g. heat pumps, air conditioning) towards increasing compactness and hence, progressively reduce the Reynolds number [1].

Performance evaluation of various type of heat transfer passive augmentation mechanism have been the objective of several studies in the present research group, with a focus on the effect of pipe wall corrugations and wall curvature [2, 3]. Turbulators represent another mean of increasing the heat transfer rate in high-Prandtl number fluids and among the numerous types

of turbulators available to date, twisted-tapes represent simple and effective devices employed in many industrial applications.

Although several experimental studies and correlations exist for the pressure drop and heat transfer characteristics of twisted-tapes, there are only few numerical studies concerned with the mechanism of heat transfer augmentation at low Reynolds number in the transitional regime. Hong and Bergles [4] reported one of the first available set of pressure drop and heat transfer measurements in pipes with twisted-tape inserts using water and ethylene glycol as working fluids. The flow Reynolds number based on the pipe diameter ranged from 13 to 2460 and the Prandtl number from 3 to 192. An increase of the Nusselt number up to 9 times the empty tube value was reported and a correlation based on the Reynolds and Prandtl numbers and on the tape twist-ratio was provided by the authors, but the onset of transition in the flow regime was not addressed in their study. Moreover, from the plots of friction and heat transfer data a sudden variation in measured values indicating a change in the flow regime was not clearly discernible.

A similar but more recent experimental study was reported by Agarwal and Rja Rao [5], where the pressure drop and heat transfer characteristics for the twisted-tape were investigated for both cooling and heating conditions using Servotherm oil as working fluid (Pr=195-375) up to a Reynolds number of 4000 based on the pipe diameter. The authors reported friction factors and Nusselts numbers up to 9 and 5 times higher, respectively, than in a smooth tube. A significant departure from available correlations for the laminar regime at approximately Re=500 could also be clearly noted from the plots of friction and heat transfer data, indicating the anticipated onset of the unstable regime in the pipe equipped with the twisted tape inserts.

Kaliakatsos et al [6] presented a numerical study of the flow and heat transfer in a pipe equipped with a twisted tape for Reynolds numbers in the range from 500 to 1500 based on the pipe diameter. The numerical model employed a steady and laminar formulation of the flow and energy equations and even though the predicted Nusselt number compared favorably to the correlation proposed by Hong and Bergles [4], the numerical results underestimated the heat transfer rate up to 35% for the highest Reynolds number when compared to the correlation presented in the study of Saha and Dutta [7].

A numerical study in the transitional flow regime from a Reynolds number of 800 to 2000 based on the pipe diameter using a turbulent, yet steady, formulation of the flow and energy equations was presented by Savekar et al. [8], where the k-ω model was used to to predict the flow pressure drop and heat transfer in a pipe with the twisted-tape insert. The comparison of numerical results with the measurements reported by Manglik and Bergles [9] shows increasing divergence in the predicted Nusselt number with increasing Reynolds number, presumably because of the onset of time-dependent perturbations which could be not accounted for by the steady formulation adopted in the analysis.

In this work, we present a numerical study of the friction and heat transfer characteristics for pipes equipped with twisted-tape inserts in the laminar to transitional flow regime. The computations are carried out with the open-source CFD package OpenFOAM®, where the flow and energy equations are solved using unstructured and second-order accurate finite-volume schemes. The numerical study is based on Scale Adaptive Simulations (SAS) where the k-ω SST model is employed for turbulence modeling. Using such model and low dissipation discretization schemes, we show that is possible to capture the laminar to turbulent transition in the flow regime and provide an accurate prediction of the increased pressure drop and heat transfer associated with the twisted-tape inserts. The paper is organized as follows: in Section 2 the numerical model adopted in the analysis is presented. An overview of turbulence modeling is given in Section 3, with particular emphasis on the SAS model. The validation of the numerical model is presented in Section 4, where the estimated friction factor and Nusselt number are compared to measurements performed in a dedicated test rig. Additional insights on the laminar

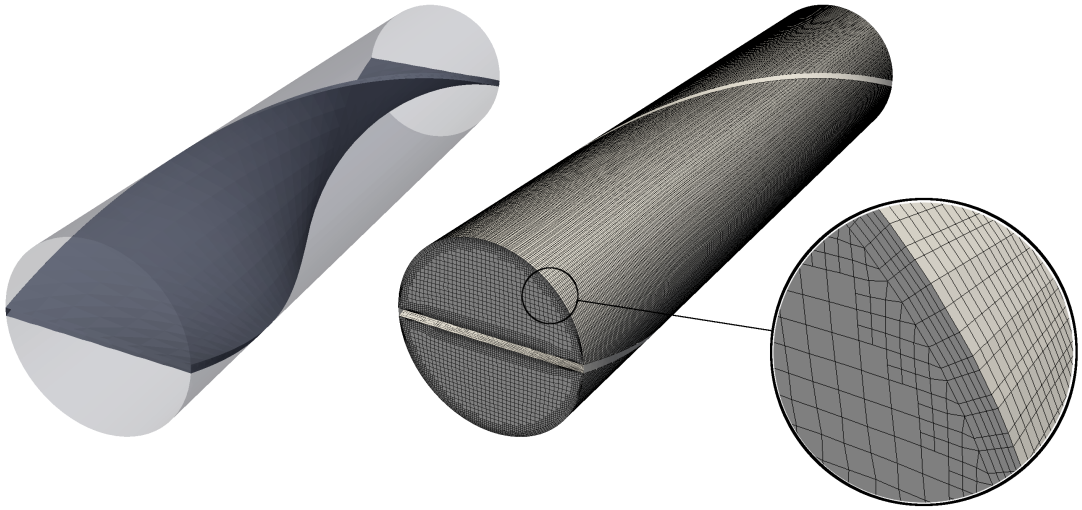

Figure 1. Numerical model of the pipe with twisted-tape insert: left, model geometry; right, computational grid; detail, close-up view of the near-wall mesh structure and resolution.

to turbulent flow transition and on the heat transfer augmentation mechanism are provided in Section 5. Conclusions and final remarks are reported at the end of the paper.

2. Numerical model

The numerical model adopted in the present study, shown in Fig. 1, consists of a single periodic module of a smooth pipe equipped with the twisted-tape, corresponding to a 180 deg rotation of the turbulator, where fully-developed flow conditions are assumed for the velocity and temperature fields. The tape is characterized by a twist-ratio $y = H/D$, where H is the pitch for 180-deg rotation of the tape and D the pipe diameter, of 4.44. In the present model, the tape is in perfect contact with the pipe wall, thus forming two separate half-sections in the pipe. The flow Reynolds number, based on the pipe diameter, ranges from 210 to 3100, whereas the Prandtl number of the working fluid, evaluated at film temperature, is 45. Because of the short length of the periodic module with respect to the pipe diameter, the variation of the flow bulk temperature is minimal and thus the temperature dependence in the properties of the working fluid is neglected in the simulations.

The following RANS formulation of flow and energy equations are solved in the simulations using the open-source finite-volume code OpenFOAM®:

$$\frac{\partial U_i}{\partial x_i} = 0 \tag{1}$$

$$\frac{\partial U_i}{\partial t} + \frac{\partial U_i U_j}{\partial x_j} = -\frac{1}{\rho}\frac{\partial P}{\partial x_i} + \nu\frac{\partial^2 U_i}{\partial x_j \partial x_j} - \frac{\partial}{\partial x_j}(\overline{u_i u_j}) \tag{2}$$

$$\frac{\partial T}{\partial t} + \frac{\partial U_j T}{\partial x_j} = \alpha\frac{\partial^2 T}{\partial x_j \partial x_j} - \frac{\partial}{\partial x_j}(\overline{u_j \theta}), \tag{3}$$

where uppercase and lowercase denote mean and fluctuating values, respectively. The $\overline{u_i u_j}$ and $\overline{u_j \theta}$ terms in Eq. (2) and (3) represent the Reynolds stress tensor and the turbulent heat

flux, respectively, and require modeling in the framework of RANS simulations. In the present work, the turbulent heat flux is approximated using the eddy-diffusivity model:

$$\overline{u_j\theta} = -\alpha_t \frac{\partial T}{\partial x_j} = -\frac{\nu_t}{Pr_t}\frac{\partial T}{\partial x_j}, \tag{4}$$

where ν_t and $Pr_t = \nu_t/\alpha_t$ denote the eddy-viscosity and the turbulent Prandtl number, respectively, and α_t the eddy-diffusivity. The standard value for wall-bounded turbulent flows of Pr_t of 0.9 is employed in the simulations, whereas the the eddy-viscosity is obtained via the $k-\omega$ SST model described in the next section.

A hex-dominant grid, also shown in Fig. 1, is employed in the computations, where boundary-layers cells aligned with the pipe surface are used to resolve the flow and thermal boundary layer at the wall. A constant and isotropic grid resolution of about $2.3\times10^{-2}D$, where D is the pipe diameter, is employed in the core region of the flow whereas the grid is isotropically refined near the tape and pipe walls to twice the resolution of the core region. The total cell count for the present grid is about 1.4M. The time-integration of the flow and energy equations is performed using a second-order implicit time-stepping scheme, whereas a limited linear scheme and a corrected linear scheme are used, respectively, for the convective and diffusive terms of the governing equations.

The boundary conditions for the velocity and temperature field at the pipe wall are of no-slip and uniform heat flux, respectively, whereas the no-slip condition and zero-flux are employed on the twisted-tape surface, meaning the heat conduction through the thickness of the tape is neglected. In the streamwise direction, the fully-developed condition for the flow field is achieved by imposing a cyclic condition between the period sections of the pipe, where the computed velocity profile at the outflow section is simply copied at the inlet section of the computational domain and the flow driven by an externally imposed constant pressure gradient.

In the case of the energy equation, however, the temperature field must be rescaled between the inlet and outlet sections of the computational domain due to the rise in the bulk temperature of the flow following from the imposed heat flux at the pipe wall. This is achieved in the present numerical model by modifying the energy equation (3) following the method proposed by Patankar et al. [10]. Figure 2 shows the validation of the implemented rescaling technique for the case of an empty pipe against the theoretical values of the friction factor and Nusselt number factors in the laminar regime $f = 64/Re$ and $Nu = 4.364$ as well as against the correlations proposed by Petukhov [15] for the turbulent regime:

$$f = (0.79\log(Re) - 1.64)^{-2} \tag{5}$$

$$Nu = \frac{(f/8(Re-1000)Pr)}{(1+12.7(f/8)^{1/2}(Pr^(2/3)-1))}, \tag{6}$$

The agreement between numerical results and theoretical values in the laminar regime is excellent and that between numerical results and Eqs. (5) and (6) also very good in the turbulent regime.

3. Turbulence modeling

The target flow regime of the present analysis is particularly challenging from the simulation standpoint because of the transition mechanism from the stable laminar regime to the fully developed turbulent flow at the highest Reynolds number. Such mechanism is in fact controlled by the balance between the stabilizing effect of the swirling motion induced by the twisted tape and the growth of perturbations associated with the onset of the turbulent flow regime [9]. Therefore, the onset of time-dependent perturbations, even at large-scales, cannot be accounted

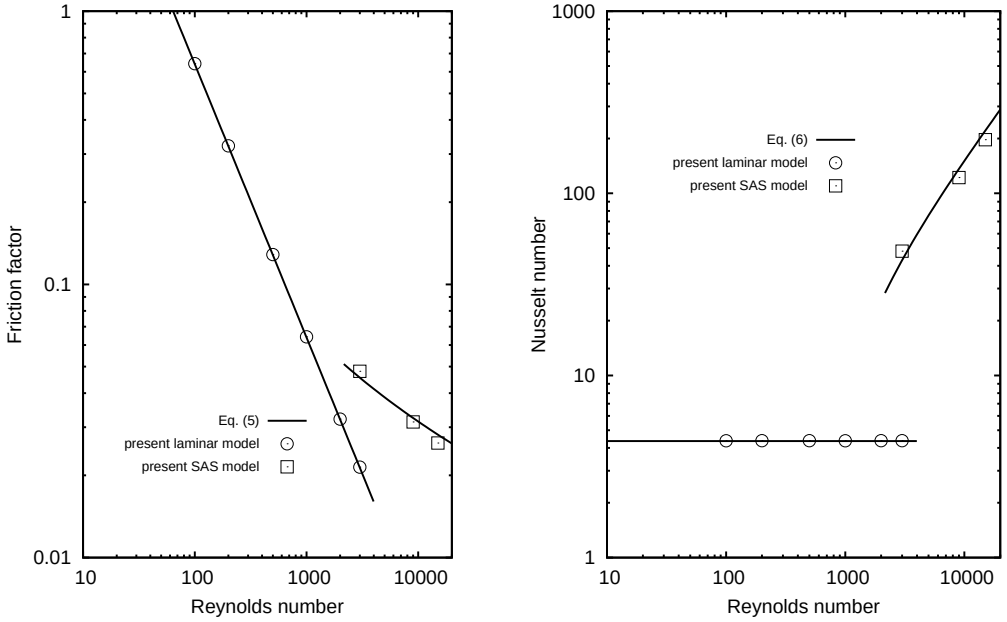

Figure 2. Validation of numerical model for laminar and turbulent flow in an empty pipe: left, friction factor; right, Nusselt number.

for in the framework of standard Unsteady-RANS (URANS) simulations. URANS operates in fact on a "separation of scales" basis and can resolve only unsteady effects characterized by very low frequencies, which are typically associated with abrupt changes in the geometry or time-dependent boundary conditions.

In the SAS formulation employed in this work, the turbulence model is formulated in a way to operate in Scale-Resolving Simulation (SRS) mode, where the model automatically balances the contribution of modelled and resolved parts of the turbulent stresses [11]. One of the more interesting features of the SAS approach is that for unstable flows as that induced by the twisted tape in the transitional regime, the model changes smoothly from a time dependent scale-resolving model to a steady scale-separating model, based on the specified time step.

The eddy-viscosity ν_t required to close the RANS formulation of governing equations (2) and (3) is obtained in the SAS model via the following relation:

$$\nu_t = c_\mu^{1/4} \sqrt{k} L, \tag{7}$$

where k is the turbulent kinetic energy and L is the integral length-scale introduced in the SRS formulation. The integral length-scale is computed via a modified form of the $k-\omega$ SST model of Menter [12], where an additional source term is introduced in the original transport equation for the turbulence frequency ω (not reported here for sake of brevity):

$$Q_{SAS} = \max\left[\rho\zeta^2 S^2 \left(\frac{L}{L_{\nu\kappa}}\right)^2 - C_{SAS}\frac{2\rho k}{\sigma_\Phi}\max\left(\frac{1}{k^2}\frac{\partial k}{\partial x_j}\frac{\partial k}{\partial x_j}, \frac{\partial 1}{\partial \omega^2}\frac{\partial \omega}{\partial x_j}\frac{\partial \omega}{\partial x_j}, 0\right)\right], \tag{8}$$

where ζ, σ_Φ and C_{SAS} are constants, S is the strain rate magnitude and $L_{\nu\kappa}$ the Von-Karman length-scale. As in the standard RANS or scale-separating formulation of the $k-\omega$ SST, the model is able to account for the viscosity-affected near-wall region of the flow without the use

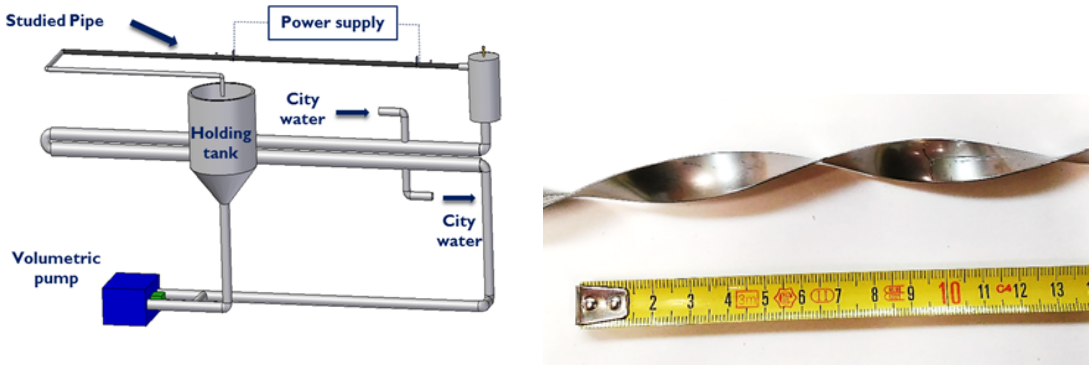

Figure 3. Experimental setup for measurements of friction factor and Nusselt number in the pipe flow with twisted-tape insert: left, schematic view of the test rig; right, twisted-tape employed in the test-rig.

of extra damping functions provided that the grid resolution is sufficient. In the present work, the grid resolution in wall-units at the first cell-centroid next to the wall ranges from y^+=0.24 to y^+=0.85 for the lowest and highest Reynolds number cases, respectively, and the viscous sublayer is therefore well-resolved. However, the thickness of the conductive thermal sublayer scales with the $Pr^{-1/2}$, leading to a near-wall resolution for the thermal field with the same grid of about y^+=1.6 to y^+=5.7 for the lowest and highest Reynolds number cases, respectively. Nonetheless, the validation study presented in Fig. 2 shows that the reduced grid resolution in the case of the energy equation is not such to limit the accuracy of present results.

The $k-\omega$ SST SAS model has been tested in numerous complex flow configurations [13] and proved to be effective in presence of instabilities associated with large separated zones or vortical instabilities, as in the case of pipe flows with twisted-tape inserts. Note that results for the friction factor and Nusselt number obtained with a laminar formulation of the numerical model are also reported for the Reynolds number range from 210 to 910 for sake of comparison with the SAS model.

4. Experimental validation of the numerical model

The validation of the numerical model for the pipe with the twisted-tape insert is carried out by comparing the predicted friction factor and Nusselt number factors with measurements performed in a dedicated test rig, shown in Fig. 3. The experimental tests are performed by adopting a stainless steel type AISI 304 tube fitted with the twisted tape. The pipe is 3 m long and presents a wall thickness of 1 mm and an internal diameter of 13.5 mm. The test section is inserted horizontally in a loop, which is completed by a secondary heat exchanger fed with city water enabling to keep the working fluid temperature constant at the tube's inlet.

The working fluid is conveyed by a volumetric pump to a holding tank from which it enters the test section equipped with fin electrodes connected to a power supply (type HP 6671A) working in the ranges 0−8 V and 0−220 A. This setup allows investigating the heat transfer performance of the tube under the prescribed condition of heat generated by Joule effect in the wall. By neglecting the changes in the local wall resistivity due to the cold working process, changes in the geometry and the effect of heat conduction in the wall, this heating condition well approximates the constant heat flux boundary condition at the fluidwall interface. The whole length of the heat transfer section was thermally insulated to minimize the heat exchange to the environment. The wall temperature was measured through 40 type T thermocouples, previously calibrated and connected to a multichannel ice point reference (type KAYE K170- 50C). Regarding the

wall temperature, the sensors are attached at different circumferential locations to the external tubes surface and at different axial locations along the heated section. The inlet temperature is measured by a thermocouple probe placed on the tubes wall upstream the start of the heating section. The bulk temperature at any location in the heat transfer section was calculated from the power supplied to the tube, which is assumed distributed uniformly per unit length over the heat transfer surface area, and by taking into account for the heat losses through the insulation. The outlet temperature is also monitored by placing a thermocouple at the end of the heated section.

The heat losses towards the environment are estimated from a preliminary calibration of the apparatus. Volumetric flow rates are obtained by measuring the time needed to fill a volumetric flask placed at the outlet of the test section. The data acquisition system consisted essentially of a high precision multimeter (type HP 3458A) connected to a switch control unit (type HP 3488A) driven by a Personal Computer. Pressure drops throughout the section fitted with twisted tapes are measured in isothermal conditions by a Rosemount-3051S differential pressure transducer. A 40% mixture of water and ethylene glycol is used as working fluid in the Reynolds number range 210-3100. In the temperature range characterizing the experimental conditions the Prandtl number of the working fluid varied in the range 44-51.

Figure. 4 shows the comparison of numerical results with measured data from the test rig and with correlations available from the experimental study of Agarwal and Raja Rao [5]:

$$f = 19.48(Re)^{-0.6519}(y)^{-0.6281} \quad (9)$$

$$Nu = 0.725(Re)^{0.568}(y)^{-0.788}(Pr)^{1/3}, \quad (10)$$

The agreement with measurements is very good for the Nusselt number, whereas the numerical model under-predicts to some extent the friction factor. The trend in the predicted pressure drop and heat transfer characteristics is overall in good agreement between the numerical model and the reference data, where the measured friction factor and Nusselt number factors are found in very good agreement with the existing correlation in the literature. Moreover, the comparison of numerical results obtained with the laminar and the SAS model suggests that the onset of the transitional regime affects the heat transfer rate to a greater extent than the pressure drop.

5. Flow and temperature fields analysis

The overall good agreement between the computed friction factor and Nusselt number against the experimental measured and reference data demonstrates the capability of the present numerical model to predict the characteristics of the pipe flow with the twisted-tape insert from the laminar to the transitional regime. In this section, such characteristics are illustrated and discussed in more detail with the help of contour plots and time-histories of the computed velocity and temperature fields.

In Fig. 5, the contour plots of velocity components and temperature on a cross-section located halfway of the periodic module are shown for increasing values of the Reynolds number. At Re=496, the instantaneous axial velocity u_z/U_b features two loci of stable and fast moving fluid on the outer side of the pipe half section with respect to the bending direction of the twisted-tape. The high-speed flow is pushed by centrifugal forces acting outwards from the inner side of the pipe, where slow moving fluid resides. With the increase in the Reynolds number, the contour plots show clearly how the flow instability originates from the low speed flow, where the negative radial pressure gradient has a destabilizing effect promoting the growth of perturbations in the flow. The flow instability propagates from the inner side to the outer side of the pipe half section with further increase in the Reynolds number, eventually determining the breakdown of the high-speed flow regions at the highest values.

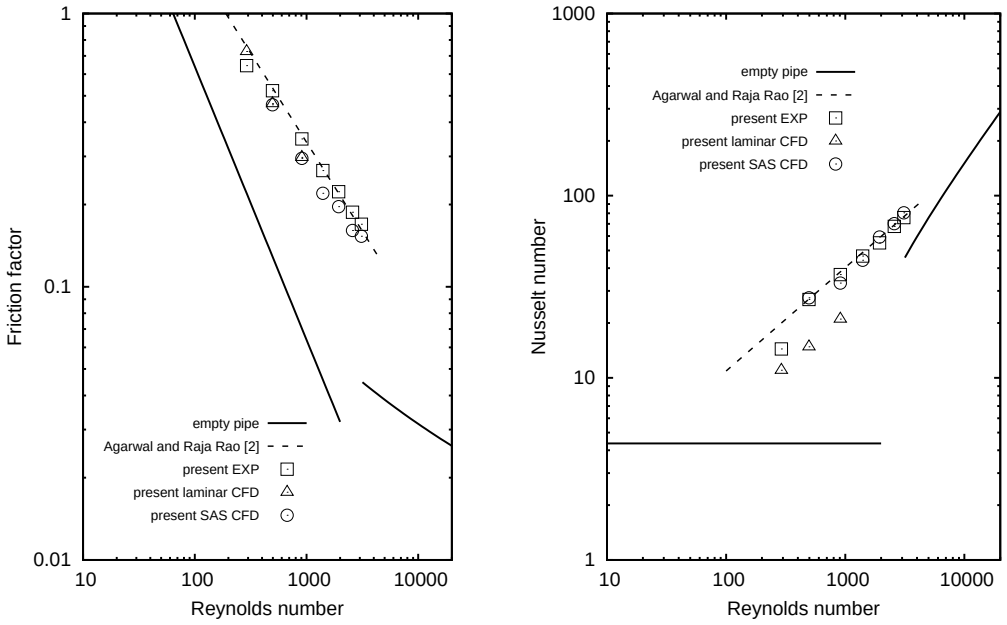

Figure 4. Validation of numerical results against measured data and available correlations for pipe flow with twisted-tape insert: left, friction factor; right, Nusselt number.

The contours of instantaneous swirl velocity $(u_x^2 + u_y^2)^{\frac{1}{2}}/U_b$ are also reported in Fig. 5. In the fully stable flow regime, the magnitude of the swirl flow is about 20% of the flow bulk velocity and the swirl flow is almost evenly distributed across each of the pipe half sections, with the peak in swirl velocity located about halfway between the pipe wall and the twisted tape surface along the radius. Because of the increasing dominance of centrifugal forces with increasing Reynolds numbers, the magnitude of the swirl flow reaches a maximum of about 35% of the bulk velocity at Re=3100. Moreover, the peak in swirl velocity moves towards the pipe wall while the uniform distribution of the swirl flow is replaced by several local maxima due to the flow instability taking place within the pipe.

The change in the flow structure due to the onset of the flow instabilities is reflected in the contour plots of normalized temperature $(T - T_w)/(T_w - T_b)$ in Fig. 5, where T_w is the average temperature of the pipe wall and T_b the flow bulk temperature. Within the stable flow regime at Re=496, the temperature distribution in each of the pipe half section features a cold fluid region corresponding to the high-speed flow in the outer part of the pipe as well as a secondary cold spot located in the inner region of the pipe occupied by the flow moving at low speed. As the Reynolds number is increased and the flow instability takes place, the two cold spots start to blend together thanks to the enhanced mixing associated with the onset and growth of perturbations in the flow. Once the turbulent mixing takes place the cold fluid is also able to penetrate the contact edge between the twisted-tape and the pipe, a region where the heat transfer rate is significantly decreased in the laminar and stable regime.

In order to better highlight the onset of the transition regime in the flow, Fig. 6 presents the time-history of the spanwise velocity component for increasing Reynolds numbers from a probe located at the center of one of the pipe half sections. At Re=496, the flow appears to be perfectly stable after the the initial oscillations due to the simulation start up from a zero velocity initial conditions, indicating that perturbations induced by the twisted-tape are damped

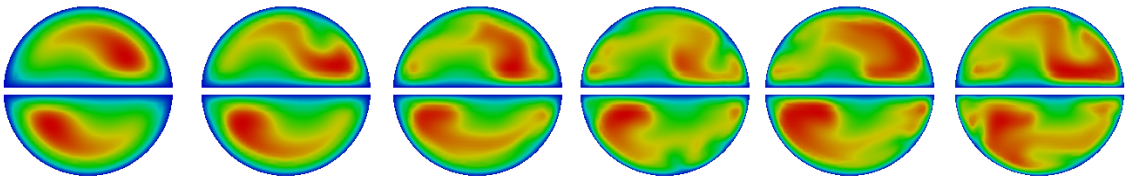

(a) Normalized axial velocity

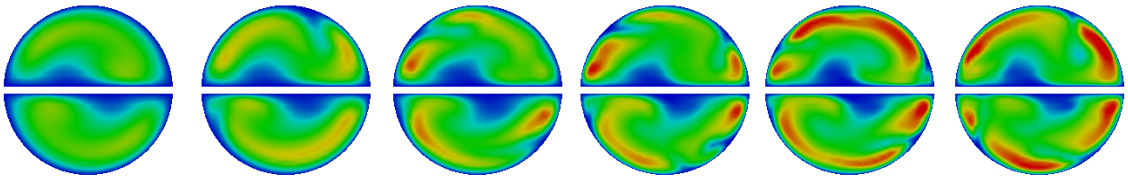

(b) Normalized swirl velocity

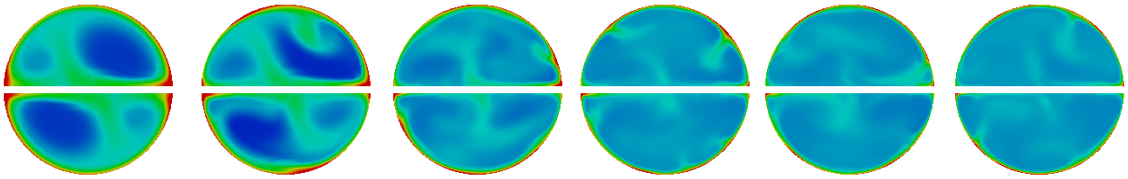

(c) Normalized temperature

Figure 5. Contours of flow and temperature field variables for increasing values of the Reynolds number: from left to right; Re=496, Re=910, Re=1400, Re=1940, Re=2580, Re=3100; from top to bottom; contours of normalized axial velocity $u_z/U_b = 0 \div 1$, contours of normalized swirl velocity $(u_x^2 + u_y^2)^{\frac{1}{2}}/U_b = 0 \div 0.35$, contours of normalized temperature $(T - T_w)/(T_w - T_b) = -1.25 \div 0$.

within the flow. By increasing the Reynolds number to 910, the recorded time history presents weak instabilities that are still dissipated within the simulated time window.

At Re=1400, however, an initial train of periodic oscillations with period $T = 4H/U_b$, where U_b is the flow bulk velocity, develops at the simulation start up anticipating the transition to a turbulent regime at $15H/U_b$. When the Reynolds number is further increased, the onset of transition occurs shortly after the start up of the simulation and the recorded time history exhibits fluctuations of increasingly larger amplitude.

6. Conclusions

In this paper, we presented a numerical study of the fully-developed flow in a pipe with twisted-tape inserts in the laminar to transitional flow regime. The simulations were carried using the

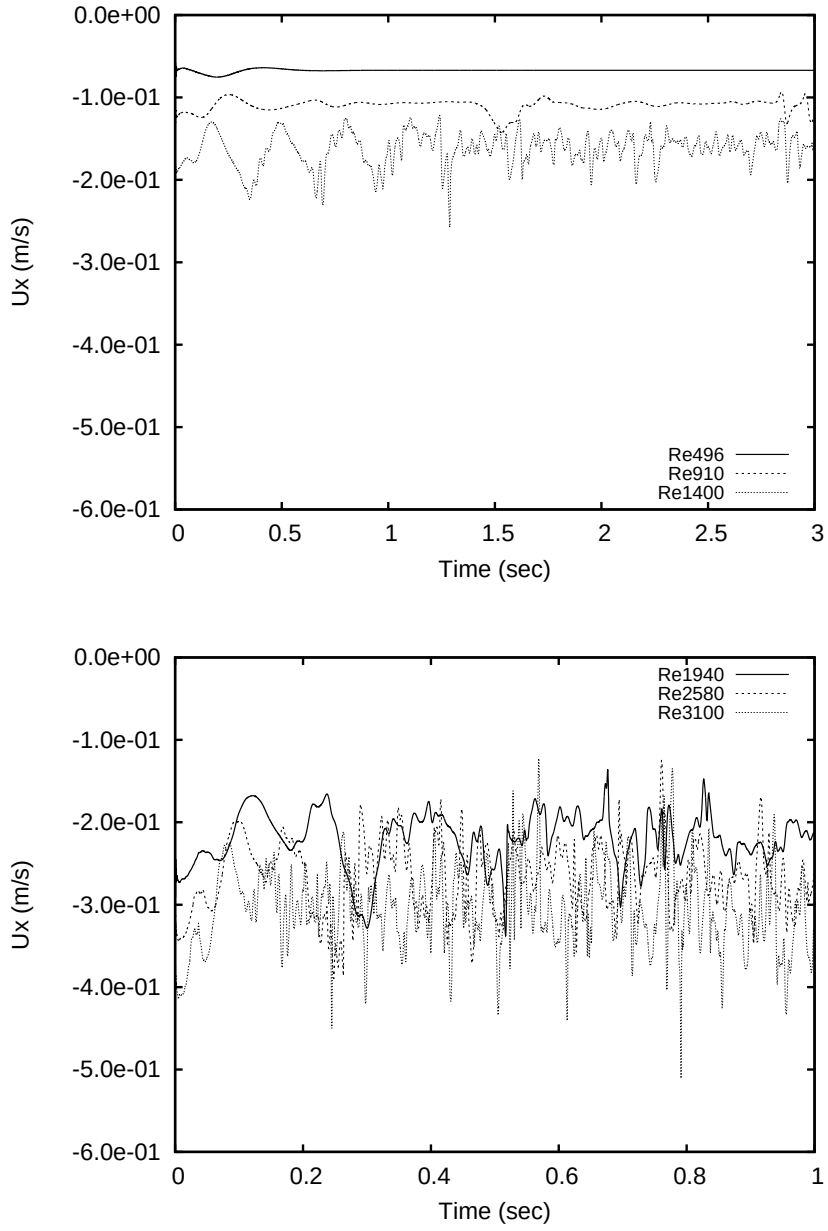

Figure 6. Time history of the spanwise velocity from a probe monitor located at the center of one of the two pipe half-sections: top, Re=469, 910, 1400; bottom, Re=1940, 2580, 3100.

open source code OpenFOAM®, based on the unstructured finite-volume scheme method, and turbulence modeling performed in the framework of Scale-Adaptive Simulations (SAS), where a modified formulation of the $k-\omega$ SST model is used to close the flow and energy RANS equations. Using SAS and low-dissipation discretization schemes, the present study shows that it is possible to capture the transition from the laminar regime to the pulsating or pseudo-laminar flow regime induced by the twisted-tape at low Reynolds numbers, as well as the transition to moderate turbulent regime at the higher, yet non-turbulent for smooth pipes, range of Reynolds numbers.

The numerical model has been validated against experimental measurements carried out in a dedicated test rig as well as against available correlations for the present flow setup, showing general good agreement with the reference data. The friction factor and Nusselt number, characterizing the pressure drop and heat transfer rate of the flow, are found increased up to 4 to 7 times and 6 to 15 times, respectively, of the values for an empty pipe, indicating that twisted-tapes are able to enhance the heat transfer performance without compromising the overall efficiency due to a significant increase in the requested pumping power.

A detailed analysis of flow and temperature fields across the transitional regime shows that the onset and growth of turbulent fluctuations occur between a Reynolds number between 910 and 1400 based on the pipe diameter. Fully-turbulent flow conditions are established beyond Re=1940, where the heat transfer rate approaches that provided by available correlations for turbulent flows in empty pipes.

Since the SAS formulation operates at a computational costs significantly lower than Direct Numerical Simulations (DNS) or Large-Eddy Simulations (LES), the present work shows that the present model as a good candidate to perform numerical simulations in similar flow conditions for other type of devices for passive heat transfer enhancement.

Acknowledgments

This work was partially supported by the Emilia-Romagna Region (POR-FESR 2014-2020: "Progetto HEGOS - nuove pompe di calore per l'Harvesting EnerGeticO in Smart buildings" and "Progetto Nuovi paradigmi per la progettazione, costruzione ed il funzionamento di macchine e impianti per l'industria alimentare").

References

[1] Reay D A, Hesselgreaves J E and Law R 2001 *Compact Heat Exchangers: Selection, Design and Operation* (Oxford: Pergamon press)
[2] Rainieri S, Bozzoli F and Pagliarini G 2012 *Int. J. Heat Mass Transf.* **55** 498
[3] Rainieri S, Bozzoli F, Cattani L and Pagliarini G 2013 *Int. J. Heat Mass Transf.* **59** 353
[4] Hong S W and Bergles A E 1976 *J. Heat. Trans.-T ASME* **98** 251
[5] Agarwal S K and Raja Rao M 1996 *Int. J. Heat Mass Transf.* **39** 3547
[6] Kaliakatsos D, Cucumo M, Ferraro V, Mele M, Galloro A and Accorinti F 2016 Int. J. Heat Technol. **34** 172
[7] Saha S K and Dutta A 2001 *J. Heat. Trans.-T ASME* **123** 417
[8] Savekar A, Jangid D, Gurjar M, Patil V and Sewatkar C M 2015 Proc. $2^n d$ Int. Conf. on Fluid Flow, Heat Mass Transf. *(Ottawa)* p 143
[9] Manglik R M and Bergles A E 1993 *J. Heat. Trans.-T ASME* **115** 881
[10] Patankar S V, Liu C H and Sparrow E M 1977 *J. Heat. Trans.-T ASME* **99** 180
[11] Menter F R and Egorov Y 2010 *Flow Turbul. Combust.* **85** 113
[12] Menter F R 1994 *AIAA J.* **32** 1598
[13] Menter F R and Egorov Y 2010 *Flow Turbul. Combust.* **85** 139
[14] Manglik R M and Bergles A E 1993 *J. Heat. Trans.-T ASME* **115** 890
[15] Petukhov B S 1970 *Adv. Heat Transf.* **6** 503